Digest Journal of Nanomaterials and Biostructures Vol. 9, No. 2, April - June 2014, p. 443 - 450

MICROSTRUCTURE OF THE a-C:H/W LAYERS DEPOSITED BY PLASMA ASSISTED SEQUENTIAL DEPOSITION METHOD

T. ACSENTE[a*], R. F. NEGREA[b], A. LAZEA-STOYANOVA[a], L.C. NISTOR[b], G. DINESCU[a]
[a]*National Institute for Laser, Plasma and Radiation Physics, PO Box Mg-36, Magurele, Bucharest, 077125, Romania*
[b]*National Institute for Materials Physics, Atomistilor 105,RO077125, Magurele-Bucharest, Romania*

A study regarding the microstructure of a-C:H/W mixed materials deposited by plasma assisted sequential deposition method is presented. The deposition of layers was performed by cyclic exposing a substrate, for predefined time intervals, to two deposition processes, working in alternative sequences: Magnetron Sputtering (MS) for metal deposition and Plasma Enhanced Chemical Vapor Deposition (PECVD) for carbon deposition. During the deposition the plasma parameters were kept constant while the durations of the individual MS and PECVD steps were systematically modified. The deposited samples were investigated using both transmission and scanning electron microscopy methods. Nanocomposite structures are obtained if each metal deposition step is interrupted in the island stage of the layer formation followed by coverage with a continuous layer of carbon. Multilayer structures are obtained when the full development of a continuous metallic layer is allowed. The spatial periodicity of the multilayers can be adjusted in between tens and hundreds of nanometers by proper setting the duration of substrate exposure to plasma sources.

(Received February 3, 2014; Accepted April 2, 2014)

Keywords: Sequential deposition, Carbon-metal nanocomposite, Multilayers, PECVD deposition, magnetron sputtering

1. Introduction

The properties of amorphous carbon coatings [1,2] are substantially modified by addition of different metals, resulting in mixed carbon/metal coatings, like nanocomposites (i.e. nanocrystals of metal inserted in a carbon matrix [3]) or multilayer structures (i.e. continuous layers of metal interspersed with continuous layers of carbon [4]). Carbon/metal nanocomposites coatings are used in tribological applications [3,5], in sensors, selective absorbers for solar cells [6,7], as coatings for medical implants [8] etc. Mixed carbon/metal layers are also useful as test layers for assessment of cleaning technologies for ITER (international thermonuclear experimental reactor), where they are formed due to wall erosion and are causing tritium retention [9,10,11]. The applications of metal carbon multilayers include protective coatings for magnetic recording disks [12,13], components for X-ray optics [14,15], tribology [16], etc. Plasma methods (both physical and chemical enhanced vapor deposition) are used for deposition of mixed carbon/metal layers. Nanocomposite layers are usually obtained by simultaneously addition of both metallic and carbonic components to substrate, by using for example: co-sputtering of metal and graphite targets [17,18], reactive magnetron sputtering of a metallic target [7,19], magnetron sputtering (MS) accompanied by a plasma enhanced chemical vapor deposition (PECVD) process [20], pulsed filtered cathodic arc deposition [21], ion beam sputtering [14], implantation of metallic ions

* Corresponding author: tomy@infim.ro

into deposited carbon films [22], pulsed laser deposition from a bi-component target [8], laser ablation of a graphite and of a metallic target [6], magnetron sputtering combined with pulsed laser deposition [23], etc. Still, under specific experimental conditions, instead of nanocomposites, spontaneous self-organized multilayer structures may develop at nanoscale level [17,19,21]; in these situations, the properties of the multilayers (mainly the spatial periodicity) strongly depends on the process parameters. Carbon/metal coatings are also produced by layer over layer addition of the components to the substrate (for example by alternative and sequential laser ablation of a graphite and of a metallic target [6]).

A sequential deposition method for either carbon/tungsten nanocomposite or multilayer thin films was proposed previously by us [24]. It consists in exposing repetitively the substrate, for a predefined number of times, to a MS discharge (for deposition of W) and to a PECVD discharge (for a-C:H deposition). The peculiarity of this process consist in adjusting the layers properties by a proper selection of temporal parameters (mainly the durations of metal and carbon deposition steps), while maintaining unmodified the plasma parameters (for both PECVD and MS). For long deposition steps (tens of seconds), the compositional depth profiles of the deposited layers show a periodic variation, indicating a multilayer structure. For lower duration of the deposition steps (few seconds), the deposited material consists of metal crystallites incorporated in a carbon matrix. The present study, based mainly on electron microscopy investigations, aims to identify the values of the temporal parameters leading to deposition of multilayers or to nanocomposite material.

2. Experimental

The plasma assisted sequential deposition method was presented previously in detail in [24] and [25]; for clarity we will be briefly review it here. The deposition setup (presented schematically in Fig.1) uses two plasma sources orthogonally mounted on a vacuum chamber. They are a two inches magnetron sputtering (MS) device for W deposition and a plasma enhanced chemical vapor deposition source (PECVD) for a-C:H deposition. A rotatable substrate holder, placed at the intersection of the plasma sources axes, exposes the substrate alternatively to each of the discharges for a predefined number of times (denoted with NCYC = number of cycles). A deposition cycle consists in: exposure of substrate to MS plasma for tW seconds, transport of substrate from MS to PECVD (lasting tTR seconds), exposure of substrate to PECVD plasma (lasting tC seconds) and finally, backward transport of substrate in front of the MS plasma source (lasting tTR seconds). During the corresponding deposition steps, each discharge is activated using radiofrequency power (13.56 MHz, 80 W applied to each plasma source). The plasma sources are turned off during the substrate movement. While the substrate transport is performed, the proper gaseous atmosphere, corresponding to the next deposition step, is prepared: 70sccm of Ar (grade 6.0) for MS, mixed with 5 sccm of C_2H_2 (grade 2.6) for the PECVD process. Ar is flowing continuously through the deposition chamber, while C_2H_2 is sequentially admitted and evacuated during the substrate transport. The base pressure in the deposition chamber is $5x10^{-3}$Pa, an it is establish to 2.4Pa during the metal deposition step and 2.7Pa during the a-C:H step. The substrate movement, sequential activation of plasma sources and gas admission are controlled through a computer.

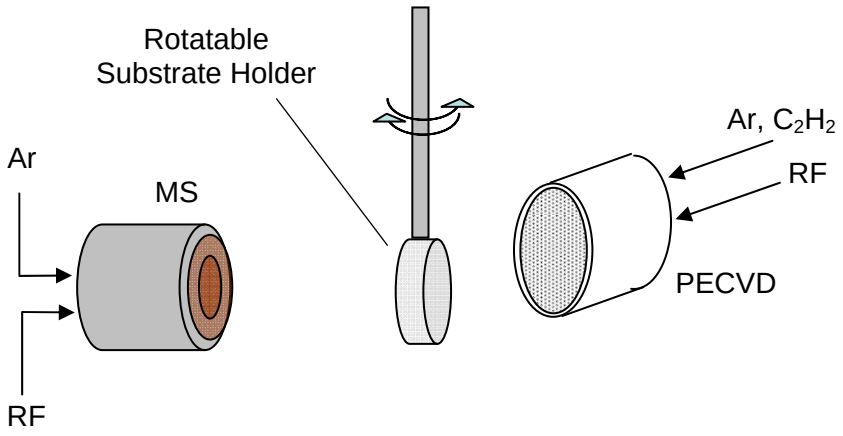

Fig.1. Schematic representation of the sequential deposition setup.

For our study, a-C:H/W layers were deposited on Si(001) substrates, considering different time values for the plasma exposure (tW, tC). Table I presents the deposited samples and their corresponding values of the temporal parameters (tW, tC, NCYC). The sample names contain the duration of exposure to plasma sources; for example 6W7C80 denotes the sample deposited using tW =6s, tC=7s, and NCYC=80. All samples were deposited using the same value of transport time, i.e. tTR=5s. All other plasma parameters (specific to MS and PECVD processes) were kept constant.

Table I. The deposited samples and the corresponding values of the temporal parameters.

Sample name	tW[s]	tC[s]	NCYC
200W400C10	200	400	10
20W40C10	20	40	10
6W7C80	6	7	80
2W11C80	2	11	80

The microstructure of the deposited layers was investigated using scanning electron microscopy (SEM) on cross sections and high resolution transmission electron microscopy (HRTEM) accompanied by the corresponding selected area electron diffraction patterns (SAED). SEM investigations were performed with a scanning electron microscope model FEI Inspect S, using an acceleration voltage of 30 kV. Cross sections for SEM investigations were obtained by cleaving the coated silicon substrates. The HRTEM studies were performed using an atomic resolution analytical JEOL JEM-ARM 200F electron microscope, operating at 200 kV. Specimens for TEM analysis were extracted under ethanol from the deposited film and transferred on holey carbon grids.

3. Results

Fig.2.a presents in cross-section the multilayer structure of a sample deposited at long times (tW an tC of hundred of seconds, 200W400C10), and Fig.2b presents the cross section of a sample deposited at shorter times (tens of seconds, 20W40C10). Both samples consist of 10 carbon layers (dark contrast) interspersed with 10 layers of tungsten based material (lighter contrast). The thickness of every layer in the sample 200W400C10 is around 100nm (the intended value); the spread of the measured values (see Fig.2.a) is most probably due to non uniform cleaving of the sample.

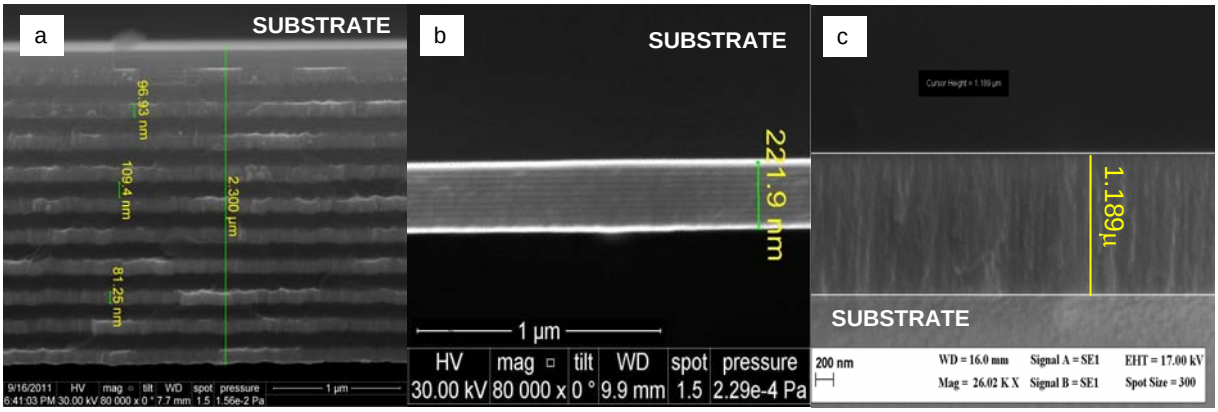

Fig.2. Cross section SEM images of samples: a) 200W400C10, b) 20W40C10 and c) 6W7C80.

Fig. 2.b clearly reveals the multilayer structure of the sample 20W40C10. It was difficult to evaluate the thickness of the individual layers because the SEM instrument was used at its resolution limit and the measurements were affected by electrostatic charging of the sample (horizontal white lines in Fig.2.b). The measured value is 219 nm, reasonable close to the intended one (200nm/layer).

For samples of a-C:H/W deposited with even lower durations of exposure to plasma (in the range of seconds), the SEM technique on the cross section suggest possible formation of a columnar like structure. This is presented in Fig.2.c for sample 6W7C80; the cross section image of the sample 2W11C80 is similar and is not presented here.

For better resolving the structural details of these samples, HRTEM investigations have been performed. Fig. 3.a shows a low magnification HRTEM micrograph of to sample 6W7C80 (tW=6s, tC=7s, tW ≈ tC), clearly revealing that the multilayer structure is still present. The SAED pattern corresponding to this micrograph (presented as inset) indicates the presence of the tetragonal WO_3 phase (JCPDS file 85-0807, a=b=0.525 nm, c=0.3915 nm) in the crystalline regions of dark contrast. Amorphous carbon is present in the lighter stripes. The WO_3 crystallites have an average dimension of 5 nm (Fig.3.b). The spatial periodicity of the multilayer structure is very close to 10nm (Fig.3.c), only twice the dimension of the WO_3 crystallite; it results that the interface between the layers is defined mainly by the WO_3 crystallites arrangement, the interlacing between WO_3 and C layers appearing to be reasonably. Indeed, the compositional profile (Fig.3.c) of the multilayer structure, obtained from the intensity line profile of the sequence C/WO_3, shows that the interfaces between the two phases are chemically diffuse. Similar interlacing between metal based and carbon layer was also observed in [14, 15] for C/W multilayer structures with nanoscale periodicity.

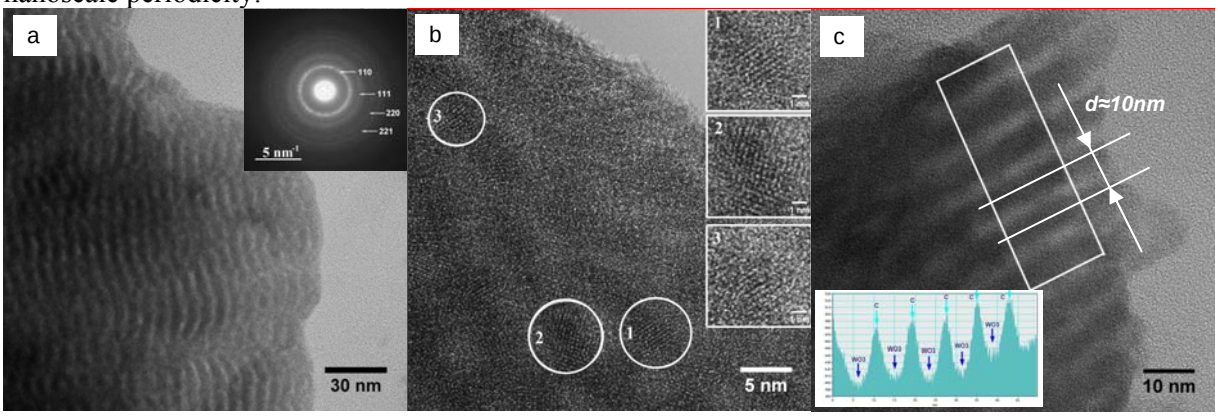

Fig. 3: HRTEM images of sample 6W7C80: a) at low magnifications the multilayer structure is revealed; the SAED pattern (inset) is indexed with the tetragonal WO_3 phase; b) at higher magnifications, lattice fringes of the encircled WO3 crystallites are visible; c) the line profile of the highlighted sequence shows the ~ 10 nm periodicity of C/WO_3 structure.

Fig.4 and Fig.5 present the HRTEM micrographs recorded in two distinct regions the sample 2W11C80 (tW=2s, tC=11s, tW << tC). The sequential character of deposition process is hardly revealed in Fig.4.a; indeed, investigations performed with higher magnification (Fig.4.b) prove that the tungsten crystallites are mostly separated from each other, and only an incipient multilayers development is apparent. The corresponding SAED pattern (not presented here) indicates that the deposited sample presents a highly amorphous character, in agreement with our previous investigation [24] performed by X-ray diffraction.

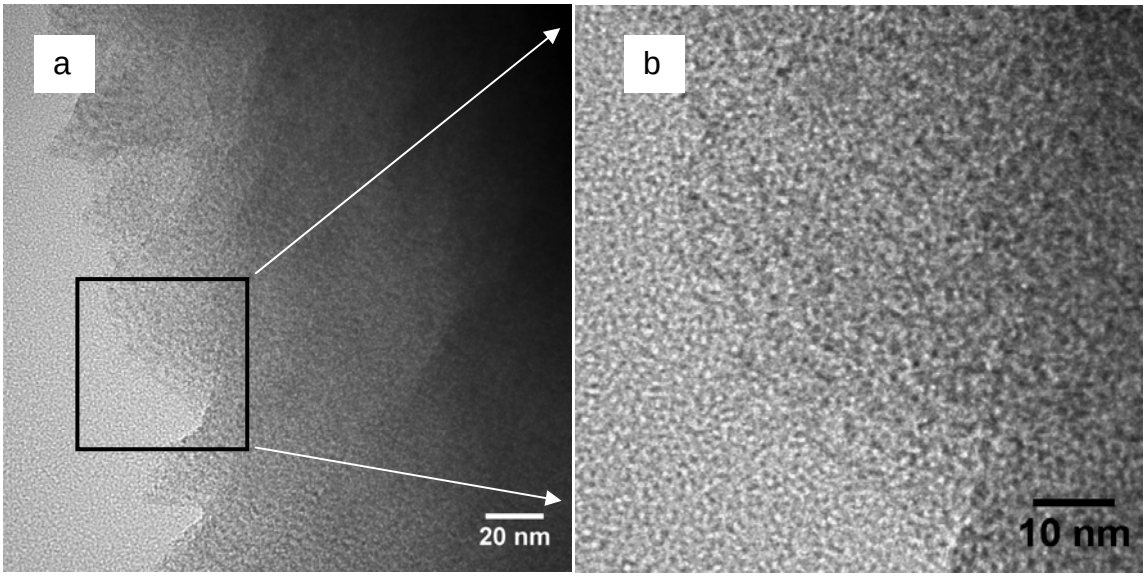

Fig.4. a) HRTEM image of sample 2W11C80 showing an area marked with a black square where the sequential character of deposition is revealed; b) the squared area at higher magnification reveals discontinuous tungsten based layers (dark contrast).

Fig.5 presents HRTEM images recorded in another area of the sample 2W11C80, where the crystallites (dark contrast) are patchy distributed in an amorphous matrix. The Fast Fourier Transform (FFT) corresponding to the HRTEM image of Fig.5.b, shows that the crystalline grains belong to the W_2(C, O) cubic phase (JCPDS file 22-0959 a=0.424 nm). Indeed, the indexed intense ring in the FFT pattern belongs to the diffraction maximum of highest intensity, which corresponds to the (111) planes of the cubic W_2(C, O) structure, presenting an interplanar distance d=0.244 nm. The dimensions of the crystallites are around 2-3nm (see Fig.5.b).

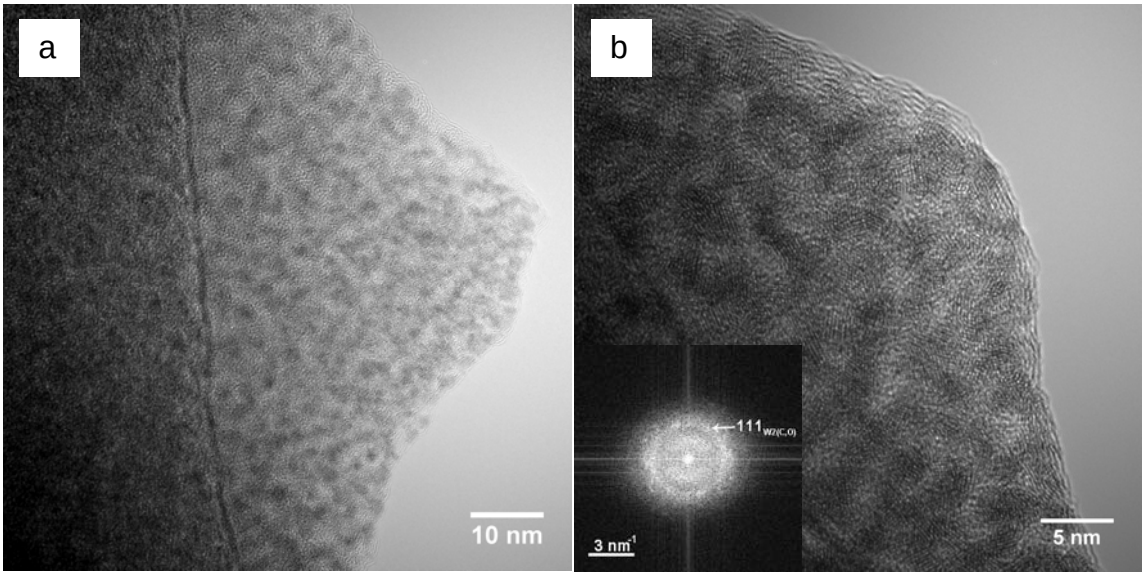

Fig.5. Low (a) and high magnifications (b) HRTEM images of the 2W11C80 sample, from a region where the crystallites are patchy distributed. In (b) the inset is the FFT of the HRTEM image showing the presence of $W_2(C,O)$ phase in the dark crystallites.

It results that sample 2W11C80 presents a nanocomposite like structure, consisting in an amorphous hydrogenated carbon a-C:H matrix in which small crystallites of tungsten compounds (carbides, oxides) are embedded.

The unexpected presence of chemical bonded oxygen in both 2W11C80 and 6W7C80 samples must to be related with the residual oxygen contained in the discharge chamber or to the impurities found in the process gases.

4. Discussions

The electron microscopy results show that, depending on the duration of the individual metal or carbon deposition steps, nanocomposite or multilayer structure can be deposited using the sequential deposition method. Thus, if during every deposition cycle, the MS step is interrupted in the island stage of the layer growth and it is subsequently followed by deposition of a continuous layer of carbon, the result will be a nanocomposite structure. It is the case of sample 2W11C80: only an incipient formation of the W continuous layer is observed in some regions of the sample during the short exposure (tW=2s) of the substrate to MS source. Increasing the duration of metal depositing step up to tW=6s (sample 6W7C80), the W based grains will coalesce forming a continuous layer; the overall result of the sequential process will be in this case a multilayer structure. Coalescence of the W based grains is favored by the high kinetic energy of the sputtered ad atoms, resulting in an increase of the islands mobility on the carbon surface. The high mobility of the metal based islands increase also their diffusion probability, explaining the mixing between layers at the interfaces (like can be observed in Fig.3.c for sample 6W7C80), similar with results reported in [15].

In view of a-C:H/W multilayer applications, especially for X rays optics, an important aspect is the chemical composition of the multilayers and of the interfaces. SAED measurements revealed chemical bonds between W and C (in $W_2(C, O)$ form) in the sample 2W11C80 (t_W=2s) while in the sample 6W7C80 (t_W=6s) they are absent (or under the detection limit). This suggest that during the MS step the C_2H_2 traces are totally consumed in a time interval very close (still higher) to t_W=2 s, the magnetron discharge continuing afterward only in the presence of the residual O_2. This result strengthens a similar conclusion obtained previously on bases of optical emission spectroscopy investigations [25]. Further increase of the deposition steps durations, up to tens/hundreds of seconds (samples 200W400C10 and 20W40C10) leads to deposition of multilayers of a-C:H/W with well-defined structure. Their spatial periodicity can be tailored between tens of nanometers up to hundreds of nanometers.

5. Conclusions

The microstructure of mixed samples of a-C:H/W deposited by plasma assisted sequential deposition method was investigated. During samples preparation the plasma generation parameters were kept constant while the temporal ones (mainly the durations of the metal magnetron sputtering and PECVD carbon deposition steps) were modified. SEM and HRTEM investigations proved that properly adjusting the duration of individual deposition steps from a few seconds up to hundreds of seconds, nanocomposite or multilayered structures can be obtained. Thus, a nanocomposite structure is formed when the metal deposition step is interrupted in the island stage of the layer growth and followed by coverage with a carbon layer. Increasing the duration of deposition steps multilayer structures can be deposited. Their spatial periodicity can be tailored in a domain ranging from ten up to hundreds of nanometers.

Acknowledgements

This work was supported by the following grants of the Ministry of National Education, CNCS – UEFISCDI: project No. 143/2012 (Priority Areas Program) and project number PN-II-ID-PCE-2012-4-0629 (IDEI) and Core Program No. PN09450103.

References

[1] Cinzia Casiraghi, John Robertson, Andrea C. Ferrari, Mater. Today, **10**, 44 (2007).
[2] C.H. Su, C.R. Lin, C.Y. Chang, H.C. Hung, T.Y. Lin, Thin Solid Films, **498**, 220 (2006).
[3] S. Vepřek, P. Nesládek, A. Niederhofer, F. Glatz, M. Jílek, M. Šíma, Surf. Coat. Technol., **108–109,** 138 (1998).
[4] David D. Allred, Qi Wang, Jesus Gonzalez-Hernandez, in Layered Structures - Heteroepitaxy, Superlattices, Strain, and Metastability, MRS Proceedings, ed. By J.E. Cunningham, B.W. Dodson, F.H. Pollak, L.J. Schowalter, Vol. 160, p.605 (Copyright © Materials Research Society 1990),
[5] C. Bauer, H. Leiste, M. Stüber, S. Ulrich, H. Holleck, Diam . Relat. Mater., **11**, 1139 (2002).
[6] N. Sbaï-Benchikh, A. Zeinert, H. Cailliérez, C. Donnet, Diam . Relat. Mater., **18**, 1085 (2009).
[7] A. Schüler, C. Ellenberger, P. Oelhafen, C. Haug, R. Brenn, J. Appl. Phys., **87**, 4285 (2000).
[8] M. Andara, A. Agarwal, D. Scholvin, et al., Diam. Relat. Mater., **15**, 1941 (2006).
[9] A. Vesel, M. Mozetič, P. Panjan, N. Hauptman, M. Klanjsek-Gunde, M. Balat-Pichelin, Surf. Coat. Tech., **204**, 1503 (2010).
[10] M. Balden, P.A. Sauter, S. Jong, C. Adelhelm, S. Lindig, M. Rasinski, T. Plocinski, Thin Solid Films **519**, 4049 (2011).
[11]M. Balden, Thin Solid Films, **519**, 4032 (2011).
[12] A. G. Ramírez, T. Itoh, R. Sinclair, J. Appl. Phys., **85**, 1508 (1999).
[13] K. Siraj, M. Khaleeq-ur-Rahman, M.S. Rafique, M.Z. Munawar, S. Naseem, S. Riaz, Appl. Surf. Sci., **257**, 6445 (2011).
[14] Kwon Su Chon, Seon Kwan Juhng , Kwon-Ha Yoon, J. Korean Phys. Soc., **54**, 23 (2009).
[15] Mohammed H. Modi, G.S. Lodha, S.R. Naik, A.K. Srivastava, R.V. Nandedkar, Thin Solid Films, **503**, 115 (2006).
[16] C. Rincón, G. Zambrano, A. Carvajal, P. Prieto, H. Galindo, E.Martínez, A. Lousa, J. Esteve, Surf. Coat. Technol., **148**, 277 (2001).
[17] D. Bíró, A. Kovács, F. Misják, T. Szüts, P.B. Barna, Surf. Coat. Technol, **180–181**, 425 (2004).
[18] E. Grigore, A.A. El Mel, A. Granier, P.Y. Tessier, Surf. Coat. Tech., **211**, 188 (2012).
[19] C. Corbella, B. Echebarria, L. Ramírez-Piscina, E. Pascual, J. L. Andújar, E. Bertran, Appl. Phys. Lett., **87**, 213117 (2005).
[20] A. A. El Mel, N. Bouts, E. Grigore, E. Gautron, A. Granier, B. Angleraud, P. Y. Tessier J. Appl. Phys., **111**, 114309 (2012).

[21] A. Pardo, J.G. Buijnsters, J.L. Endrino, C. Gómez-Aleixandre, G. Abrasonis, R. Bonet, J. Caro, Appl. Surf. Sci., **280**,791 (2013) .
[22] L. Cui, L. Guoqing, C. Wenwu, M. Zongxin, Z. Chengwu, W. Liang, Thin Solid Films, **475**, 279 (2005).
[23] M. Jelínek, T. Kocourek, Ja. Kadlec, J. Zemek, Laser Phys., **19**, 149 (2009).
[24] T. Acsente, E.R. Ionita, D. Colceag, A. Moldovan, C. Luculescu, R. Birjega, G. Dinescu, Thin Solid Films, **519**, 4054 (2011).
[25] T. Acsente, E.R. Ionita, C. Stancu, M.D. Ionita, G. Dinescu, C. Grisolia, Surf. Coat. Tech., **205**, S402 (2011).